

# Exploration of Tumor-Suppressive MicroRNAs Silenced by DNA Hypermethylation in Oral Cancer

Ken-ichi Kozaki,<sup>1,3</sup> Issei Imoto,<sup>1,3</sup> Seiki Mogi,<sup>2,4</sup> Ken Omura,<sup>2,4</sup> and Johji Inazawa<sup>1,3,5,6</sup>

<sup>1</sup>Department of Genome Medicine, <sup>2</sup>Department of Advanced Molecular Diagnosis and Maxillofacial Surgery, Hard Tissue Genome Research Center, <sup>3</sup>Department of Molecular Cytogenetics, Medical Research Institute, <sup>4</sup>Department of Oral and Maxillofacial Surgery, Graduate School, and <sup>5</sup>21st Century Center of Excellence Program for Molecular Destruction and Reconstitution of Tooth and Bone, Tokyo Medical and Dental University, Tokyo, Japan and <sup>6</sup>Core Research for Evolutional Science and Technology of Japan Science and Technology Corp., Saitama, Japan

## Abstract

In the last few years, microRNAs (miRNA) have started a revolution in molecular biology and emerged as key players in the carcinogenesis. They have been identified in various tumor types, showing that different sets of miRNAs are usually deregulated in different cancers. To identify the miRNA signature that was specific for oral squamous cell carcinoma (OSCC), we first examined expression profiles of 148 miRNAs in a panel of 18 OSCC cell lines and the immortalized oral keratinocyte line RT7 as a control. Compared with RT7, the expression of 54 miRNAs (36.5%) was frequently down-regulated in OSCC lines (<0.5-fold expression,  $\geq 66.7\%$  of 18 lines). Among these 54 miRNAs, we further analyzed four of these miRNAs (i.e., *miR-34b*, *miR-137*, *miR-193a*, and *miR-203*), located around CpG islands, to identify tumor-suppressive miRNAs silenced through aberrant DNA methylation. The expression of those four genes was restored by treatment with 5-aza-2'-deoxycytidine in OSCC cells lacking their expression. In addition, expression levels of the four miRNAs were inversely correlated with their DNA methylation status in the OSCC lines. In primary tumors of OSCC with paired normal oral mucosa, down-regulation of miRNA expression through tumor-specific hypermethylation was more frequently observed for *miR-137* and *miR-193a* than for *miR-34b* and *miR-203*. Moreover, the ectopic transfection of *miR-137* or *miR-193a* into OSCC lines lacking their expressions significantly reduced cell growth, with down-regulation of the translation of cyclin-dependent kinase 6 or E2F transcription factor 6, respectively. Taken together, our results clearly show that *miR-137* and *miR-193a* are tumor suppressor miRNAs epigenetically silenced during oral carcinogenesis. [Cancer Res 2008;68(7):2094–105]

## Introduction

MicroRNAs (miRNA) are endogenous small non-protein-coding RNAs of ~22 nucleotides. These single-strand RNAs are considered to play crucial roles in many normal cellular processes, such as proliferation, development, differentiation, and apoptosis, by regulating target gene expression through imperfect pairing with target mRNAs of protein-coding genes, inducing direct mRNA

degradation or translational inhibition (1–4). In human cancer, recent studies have shown the deregulation of miRNA expression and the contribution of miRNAs to the multistep processes of carcinogenesis either as oncogenes or tumor suppressor genes (TSG; refs. 5, 6). Tumor-specific down-regulation of subsets of miRNAs has generally been observed in various types of human cancer (7), suggesting that some of these miRNAs act as TSGs in specific tumors. Because the down-regulation of many known TSGs in human cancer has been tightly linked to the hypermethylation of CpG sites located within CpG islands with promoter activity, the same mechanism could play an important role in the silencing of tumor-suppressive miRNAs in tumors. Indeed, only a few miRNA genes were reported to be located within homozygous or hemizygous deleted regions (8–10), and several possible tumor-suppressive miRNAs, including *miR-124a* (11) and *miR-127* (12), were also reported as targets for DNA methylation for silencing in cancer cells, prompting us to screen for more tumor-suppressive miRNAs silenced through aberrant DNA methylation in a tumor-specific manner.

Oral cancer, predominantly oral squamous cell carcinoma (OSCC), is the most common head and neck neoplasm, affecting ~270,000 people worldwide in 2002 (13). In Japan, OSCC is relatively common, accounting for >5,500 deaths in 2003 (14). The carcinogenesis, including OSCC (15), is generally considered to arise through the progressive accumulation of multiple genetic abnormalities, which may impair the functions of oncogenes or TSGs that play a crucial role in the development of this disease. In addition, evidence has emerged that epigenetic mechanisms, such as altered DNA methylation patterns, play a significant role in the silencing of TSGs and contribute to malignant transformation during oral carcinogenesis (16). Recently, genome-wide screenings of DNA copy number alterations for exploring OSCC-associated oncogenes or TSGs have been reported, including by us (17–21). However, there is no report about abnormal expression of miRNA genes and their genetic or epigenetic alterations in OSCC.

We describe here the identification of tumor suppressor miRNAs, *miR-137* and *miR-193a*, frequently silenced by DNA methylation in OSCC. To explore the putative presence of DNA methylation-associated silencing of miRNAs specifically in OSCC cells, we used an approach with a series of sequential analyses. We first examined a panel of 18 OSCC cell lines and an immortalized oral keratinocyte line, RT7, for the presence of abnormal levels of expression in 148 miRNAs and then focused on four miRNAs whose down-regulated expression related to their DNA methylation status within CpG islands around them. Among four miRNAs, methylation and expression analyses using 11 primary OSCC cases with paired normal oral mucosa showed that *miR-137* and *miR-193a* show reduced expression in tumors through tumor-specific DNA methylation. Ectopic expression of *miR-137* and *miR-193a* in OSCC

**Note:** Supplementary data for this article are available at Cancer Research Online (<http://cancerres.aacrjournals.org/>).

**Requests for reprints:** Johji Inazawa, Department of Molecular Cytogenetics, Medical Research Institute, Tokyo Medical and Dental University, 1-5-45 Yushima, Bunkyo-ku, Tokyo 113-8510, Japan. Phone: 81-3-5803-5820; Fax: 81-3-5803-0244; E-mail: johinaz.cgen@mri.tmd.ac.jp.

©2008 American Association for Cancer Research.  
doi:10.1158/0008-5472.CAN-07-5194

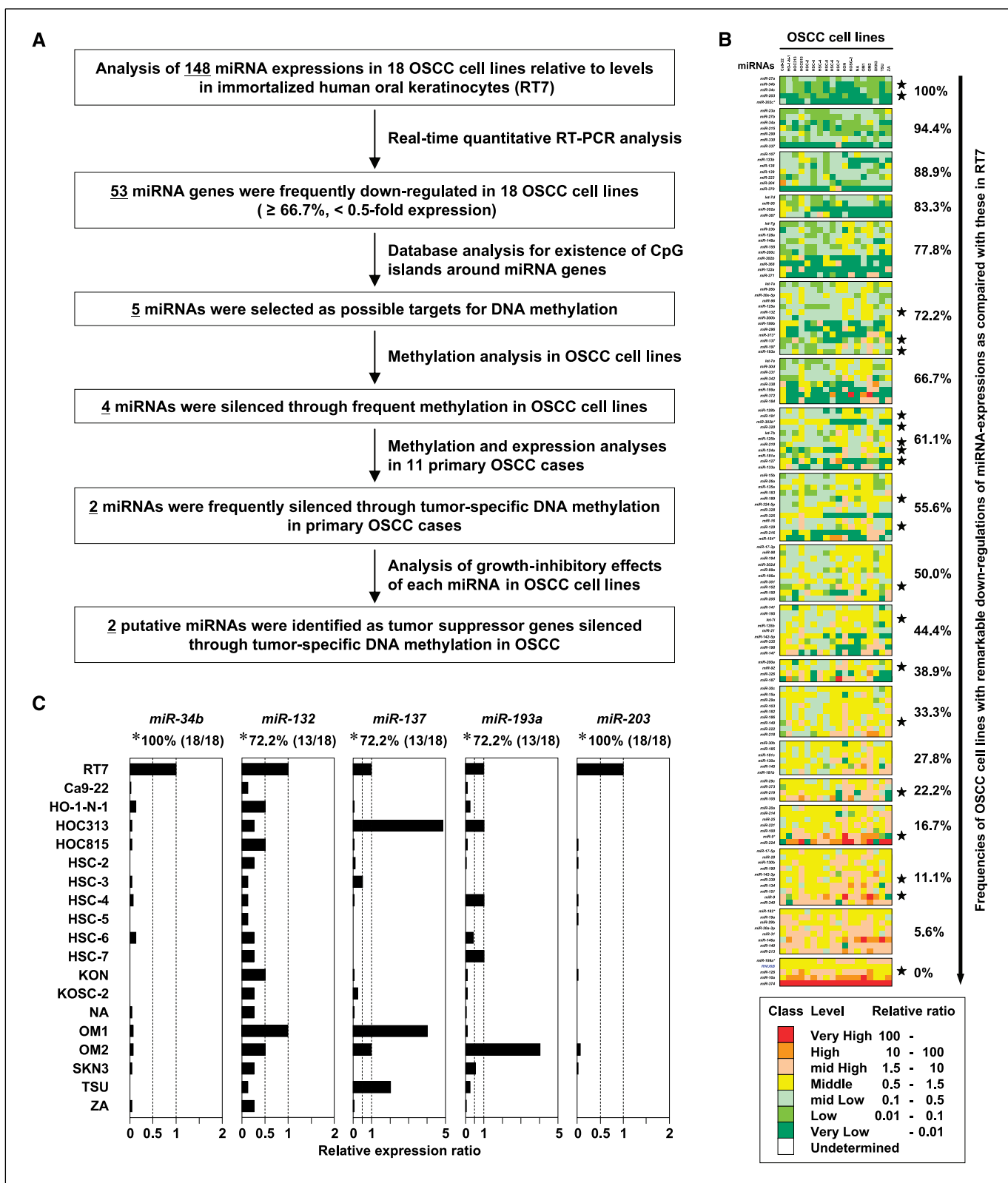


**Figure 1.** Strategy of this study and expression analysis for miRNAs in OSCC cell lines. *A*, schematic strategy for the identification of epigenetically silenced tumor suppressor miRNAs in OSCC. *B*, profiles of 148 miRNA expression in 18 OSCC cell lines relative to RT7 obtained with a Taqman MicroRNA Assays Human Panel Early Access kit. Expression levels of miRNA were based on the amount of target message relative to the *RNU6B* control to normalize the initial input of total RNA. Stars, 21 miRNAs located on/around CpG islands. RT7 cells were cultured in KGM-2 BulletKit (Cambrex) supplemented with 25% DMEM and 2.5% fetal bovine serum for 7 d. *C*, expression levels of candidate miRNAs, located on/around CpG islands, in 18 OSCC cell lines. Bar graphs in each cell line show the ratio of the expression level in each cell line to that in RT7. \*, frequencies of OSCC cell lines, in which a remarkable down-regulation of candidate miRNA expression ( $< 0.5$ -fold expression) was observed compared with that in RT7.

**Table 1.** Frequencies of OSCC cell lines with remarkable differences of miRNA expression from that in RT7 ( $\geq 66.7\%$  of OSCC cell lines)

miRNA	Locus	Frequency (%)
miRNAs frequently up-regulated in OSCC cell lines (>1.5-fold expression)		
<i>miR-374</i>	Xq13.2	100.0
<i>miR-340</i>	5q35.3	83.3
<i>miR-224</i>	Xq28	83.3
<i>miR-10a</i>	17q21.32	77.8
<i>miR-140</i>	16q22.1	77.8
<i>miR-181a*</i>	1q31.3	77.8
<i>miR-146a</i>	5q33.3	72.2
<i>miR-126</i>	9q34.3	66.7
<i>miR-31</i>	9p21.3	66.7
<i>miR-9</i>	<i>miR-9-1</i> , 1q22; <i>miR-9-2</i> , 5q14.3; <i>miR-9-3</i> , 15q26.1	66.7
<i>miR-9*</i>	<i>miR-9-1</i> , 1q22; <i>miR-9-3</i> , 15q26.1	66.7
miRNAs frequently down-regulated in OSCC cell lines (<0.5-fold expression)		
<i>miR-27a</i>	19p13.12	100.0
<i>miR-34b</i>	11q23.1	100.0
<i>miR-34c</i>	11q23.1	100.0
<i>miR-203</i>	14q32.33	100.0
<i>miR-302c*</i>	4q25	100.0
<i>miR-23a</i>	19p13.12	94.4
<i>miR-27b</i>	9q22.32	94.4
<i>miR-34a</i>	1p36.23	94.4
<i>miR-215</i>	1q41	94.4
<i>miR-299</i>	14q32.31	94.4
<i>miR-330</i>	19q13.32	94.4
<i>miR-337</i>	14q32.31	94.4
<i>miR-107</i>	10q23.31	88.9
<i>miR-133b</i>	6p12.2	88.9
<i>miR-138</i>	<i>miR-138-1</i> , 3p21.33; <i>miR-138-2</i> , 16q13	88.9
<i>miR-139</i>	11q13.4	88.9
<i>miR-223</i>	Xq12	88.9
<i>miR-204</i>	9q21.11	88.9
<i>miR-370</i>	14q32.31	88.9
<i>let-7d</i>	9q22.32	83.3
<i>miR-95</i>	4p16.1	83.3
<i>miR-302a</i>	4q25	83.3
<i>miR-367</i>	4q25	83.3
<i>let-7g</i>	3p21.1	77.8
<i>miR-23b</i>	9q22.32	77.8
<i>miR-128a</i>	2q21.3	77.8
<i>miR-148a</i>	7p15.2	77.8
<i>miR-155</i>	21q21.3	77.8
<i>miR-200c</i>	12p13.31	77.8
<i>miR-302b</i>	4q25	77.8
<i>miR-368</i>	14q32.31	77.8
<i>miR-122a</i>	18q21.31	77.8
<i>miR-371</i>	19q13.41	77.8
<i>let-7a</i>	<i>let-7a-1</i> , 9q22.32; <i>let-7a-2</i> , 11q24.1; <i>let-7a-3</i> , 22q13.31	72.2
<i>miR-26b</i>	2q35	72.2
<i>miR-30e-5p</i>	1p34.2	72.2
<i>miR-96</i>	7q32.2	72.2
<i>miR-125a</i>	19q13.33	72.2

**Table 1.** Frequencies of OSCC cell lines with remarkable differences of miRNA expression from that in RT7 ( $\geq 66.7\%$  of OSCC cell lines) (Cont'd)

miRNA	Locus	Frequency (%)
miRNAs frequently down-regulated in OSCC cell lines (<0.5-fold expression)		
<i>miR-132</i>	17p13.3	72.2
<i>miR-200b</i>	1p36.33	72.2
<i>miR-199b</i>	9q34.11	72.2
<i>miR-296</i>	20q13.32	72.2
<i>miR-373*</i>	19q13.41	72.2
<i>miR-137</i>	1p21.3	72.2
<i>miR-197</i>	1p13.3	72.2
<i>miR-193a</i>	17q11.2	72.2
<i>let-7e</i>	19q13.33	66.7
<i>miR-30d</i>	8q24.22	66.7
<i>miR-331</i>	12q22	66.7
<i>miR-342</i>	14q32.2	66.7
<i>miR-338</i>	17q25.3	66.7
<i>miR-199a</i>	<i>miR-199a-1</i> , 19p13.2; <i>miR-199a-2</i> , 1q24.3	66.7
<i>miR-372</i>	19q13.41	66.7
<i>miR-184</i>	15q25.1	66.7

cell lines lacking their expression inhibited cell growth through G<sub>0</sub>-G<sub>1</sub> arrest and caspase-mediated apoptosis, respectively, suggesting their tumor-suppressive activity. Moreover, we identified that *cyclin-dependent kinase 6 (CDK6)* and *E2F transcription factor 6 (E2F6)* were potential targets of *miR-137* and *miR-193a*, respectively, in OSCC. The present study is the first to show that epigenetic silencing of *miR-137* and *miR-193a* may play a pivotal role during oral carcinogenesis.

## Materials and Methods

**Cell lines and primary tumor samples.** Derivations and culture conditions of cell lines have been reported previously (21). To analyze the restoration of genes of interest, cells were cultured with or without 10  $\mu\text{mol/L}$  of 5-aza-2'-deoxycytidine (5-aza-dCyd) for 5 d. A total of 11 frozen primary samples were obtained from OSCC patients (T1, 0 case; T2, 10 cases; T3, 0 case; and T4, 1 case) treated at Tokyo Medical and Dental University with written consent from each patient in the formal style and after approval by the local ethics committee. The tumor-node-metastasis classification of the International Union Against Cancer was used.

**Real-time reverse transcription-PCR.** Real-time reverse transcription-PCR (RT-PCR) was performed using an ABI Prism 7500 Fast Real-time PCR System (Applied Biosystems), Taqman Universal PCR Master Mix (Applied Biosystems), Taqman Reverse Transcription kit (Applied Biosystems), Taqman MicroRNA Assays (Applied Biosystems), and Human Panel Early Access kit (Applied Biosystems) according to the manufacturer's instructions. Expression levels of miRNA genes were based on the amount of the target message relative to that of the *RNU6B* transcript as a control to normalize the initial input of total RNA.

**Methylation analysis.** Genomic DNA was treated with sodium bisulfite and subjected to PCR using primer sets designed to amplify regions of interest (Supplementary Table S1). For the combined bisulfite restriction analysis (COBRA), PCR products were digested with *Bst*UI or *Taq*I, which recognizes sequences unique to methylated alleles but cannot recognize unmethylated alleles, and electrophoresed (22). For the bisulfite sequencing analysis, the PCR products were subcloned and then sequenced.

**Transfection with synthetic miRNAs.** Pre-miR miRNA Precursor Molecule (10 nmol/L; Ambion) mimicking *miR-137* or *miR-193a*, or control

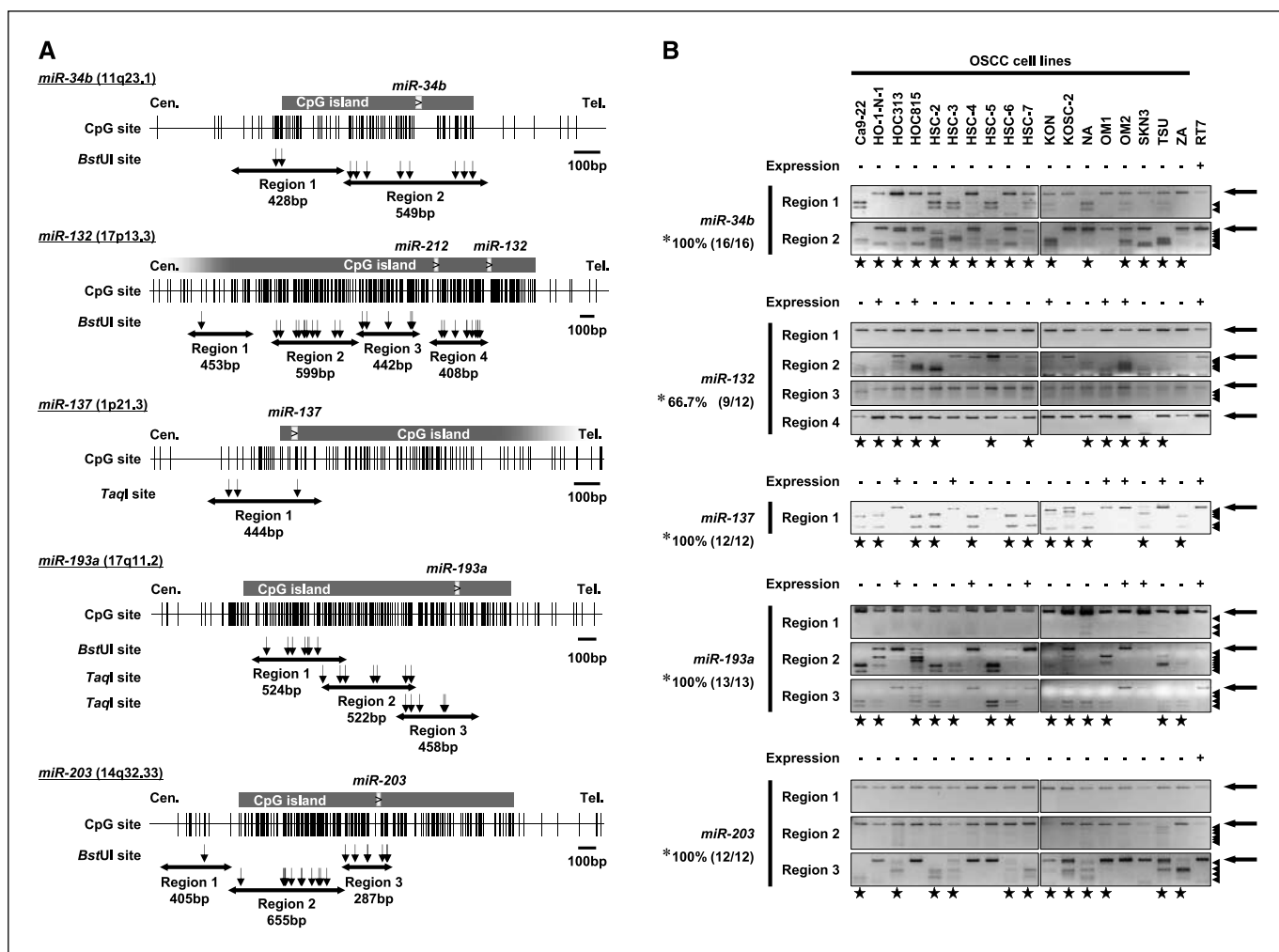


**Figure 2.** Analysis for the correlation between methylation status and expression of five candidate miRNA genes in OSCC cell lines. **A**, maps of miRNAs, CpG islands, CpG sites, and PCR products used for COBRA and bisulfite sequencing. *Dark gray box*, CpG islands; *light gray box*, miRNAs; *vertical tick marks*, CpG sites; *horizontal bars with arrowheads*, PCR product; *vertical arrows*, restriction enzyme sites. PCR product sizes (*horizontal arrows*) are as follows: *miR-34b* region, 1,428 bp (restricted by *Bst*UI); *miR-34b* region, 2,549 bp (restricted by *Bst*UI); *miR-132* region, 1,453 bp (restricted by *Bst*UI); *miR-132* region, 2,599 bp (restricted by *Bst*UI); *miR-132* region, 3,442 bp (restricted by *Bst*UI); *miR-132* region, 4,408 bp (restricted by *Bst*UI); *miR-137* region, 1,444 bp (restricted by *Taq*I); *miR-193a* region, 1,524 bp (restricted by *Bst*UI); *miR-193a* region, 2,522 bp (restricted by *Taq*I); *miR-193a* region, 3,458 bp (restricted by *Taq*I); *miR-193a* region, 1,405 bp (restricted by *Bst*UI); *miR-203* region, 2,655 bp (restricted by *Bst*UI); and *miR-203* region, 3,287 bp (restricted by *Bst*UI). **B**, the results of COBRA in OSCC cell lines and RT7. Expression pattern of candidate miRNA genes in 18 OSCC cell lines is indicated above the results of COBRA. *Arrows*, unmethylated alleles; *arrowheads*, methylated alleles; *stars*, samples detected the restricted fragments from methylated alleles. \*, frequencies of OSCC cell lines, in which DNA methylation accorded with a remarkable down-regulation of each candidate miRNA expression. Note that the denominator is the number of OSCC cell lines, in which restricted fragments from methylated alleles were detected, and the numerator is the number of OSCC cell lines, in which both DNA methylation around miRNA genes and a down-regulation of expression were detected.

nonspecific miRNA (Pre-miR Negative Control #1, Ambion) was transfected into OSCC cell lines using Lipofectamine RNAiMAX (Invitrogen) according to the manufacturer's instructions. The numbers of viable cells 24 to 72 h after transfection were assessed by the colorimetric water-soluble tetrazolium salt (WST) assay (Cell Counting Kit-8, Dojindo Laboratories). Results were normalized to the cell numbers in control cells transfected with nonspecific miRNA. Cell cycle was evaluated 48 h after transfection by fluorescence-activated cell sorting (FACS) analysis as described elsewhere (21). Apoptosis was detected 24 h after transfection by enzymatic labeling of DNA strand breaks using a terminal deoxynucleotidyl transferase-mediated dUTP nick end labeling (TUNEL) staining kit (MEBSTAIN Apoptosis Kit Direct, MBL) according to the manufacturer's directions. To evaluate the effects of caspase inhibitors on miRNA-induced growth inhibition, cells were treated with caspase-3 inhibitor zDEVD-fmk, caspase-8 inhibitor zETD-fmk, general caspase inhibitor zVAD-fmk (R&D Systems), or vehicle 1 h before transfection, and the numbers of viable cells were assessed 48 h after transfection by WST assay.

**miRNA target predictions, Western blotting, and luciferase activity assay.** Predicted targets for *miR-137* or *miR-193a* and their target sites (Supplementary Table S2) were analyzed using miRanda,<sup>7</sup> TargetScan,<sup>8</sup> and PicTar.<sup>9</sup>

The protein expression levels of predicted targets in transiently transfected cells were analyzed 48 h after transfection by Western blotting using anti-E2F6, anti-KRAS, anti-myeloid cell leukemia 1 (MCL1), anti-NCOA2/TIF2, anti-PTK2/FAK (Abcam), anti-CDK6 (Cell Signaling Technology), anti-MYCIN (Santa Cruz Biotechnology), and anti- $\beta$ -actin monoclonal antibodies (Sigma) and anti-Bcl-2, anti-Bcl-X<sub>L</sub> (Abcam), and anti-E2F1 rabbit polyclonal antibodies (Santa Cruz Biotechnology).

<sup>7</sup> <http://microrna.sanger.ac.uk/sequences/index.shtml>

<sup>8</sup> <http://www.targetscan.org/>

<sup>9</sup> <http://pictar.bio.nyu.edu/>

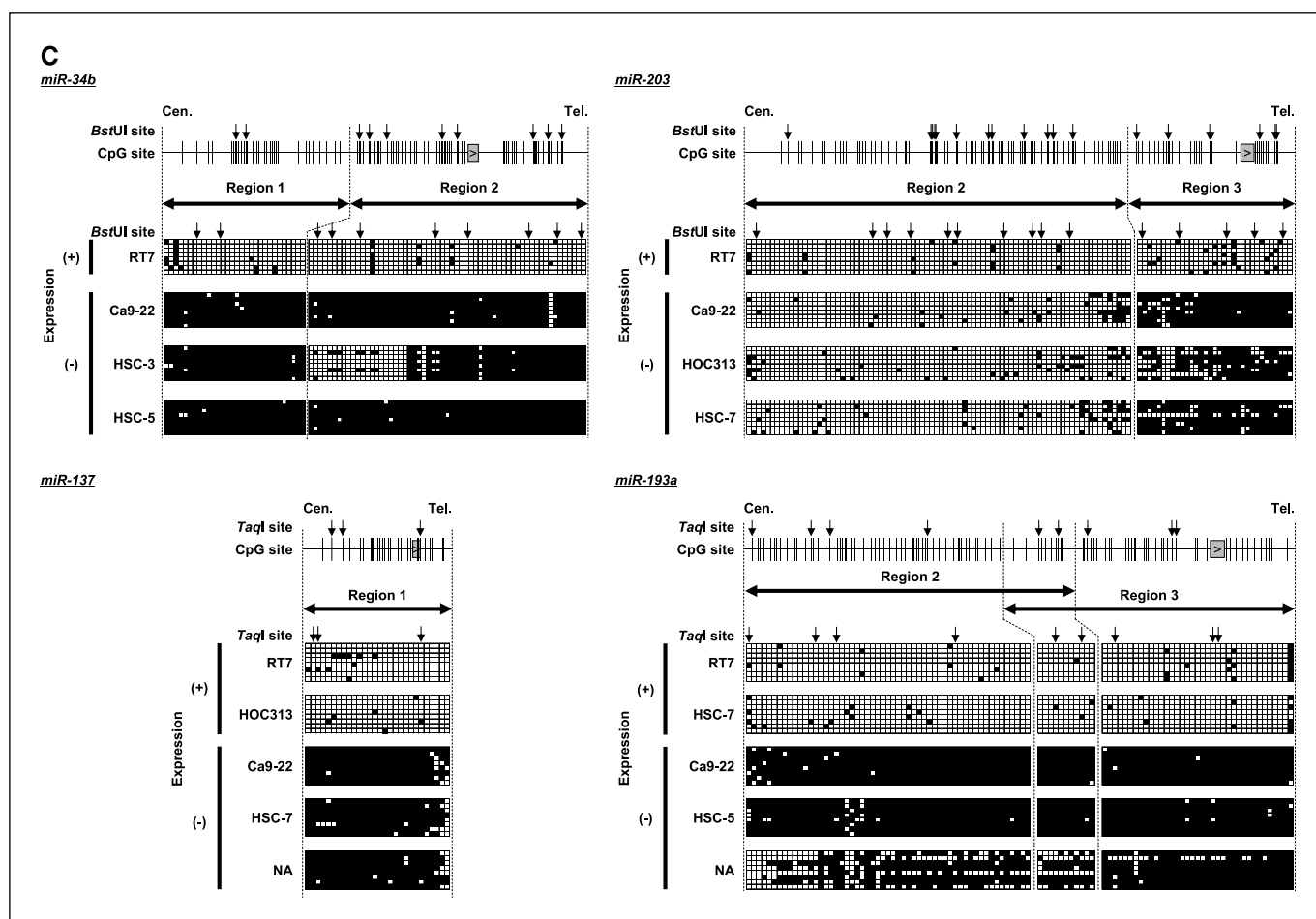


**Figure 2 Continued. C.** bisulfite sequencing of RT7 and representative OSCC cell lines with (+) or without (-) candidate miRNA expression in regions within/around candidate miRNA genes. Maps of miRNAs, CpG sites, and PCR products used for COBRA and bisulfite sequencing are indicated above the results of bisulfite sequencing. Light gray box, miRNAs; vertical tick marks, CpG sites; horizontal bars with arrowheads, PCR product; vertical arrows, restriction enzyme sites. Open and filled squares represent unmethylated and methylated CpG sites, respectively, and each row represents a single clone.

Luciferase constructs were made by ligating oligonucleotides containing the 3'-untranslated region (UTR) target sites of *CDK6*, *E2F6*, *MCL1*, *NCOA2/TIF2*, and *PTK2/FAK* (Supplementary Table S3) into downstream of the luciferase gene in pMIR-REPORT luciferase vector (Ambion). An equal amount (400 ng) of each reporter construct and 10 nmol/L of Pre-miR miRNA Precursor Molecule mimicking *miR-137* or *miR-193a*, or Pre-miR Negative Control #1 was introduced into cells with 20 ng of an internal control vector (pRL-hTK, Promega) using Lipofectamine 2000 (Invitrogen). Firefly luciferase and *Renilla* luciferase activities were each measured 48 h after transfection using the Dual-Luciferase Reporter Assay System (Promega); relative luciferase activities were calculated and normalized versus *Renilla* luciferase activity. Each transfection was repeated twice in triplicate.

**Statistical analysis.** Differences between subgroups were tested with the Mann-Whitney *U* test.

## Results

**miRNA expression profiles in 18 OSCC cell lines relative to those in RT7.** The present study, strategy and partial results of which are shown in Fig. 1A, was designed to identify tumor suppressor miRNAs silenced by tumor-specific DNA methylation in OSCC. To identify differentially expressed miRNAs in OSCC, we first performed expression profiling for 157 mature miRNAs in 18

OSCC cell lines and their normal counterpart RT7, an immortalized human oral keratinocyte line, using a highly sensitive Taqman MicroRNA Assays Human Panel Early Access kit (Fig. 1B). Among 157 miRNAs, *miR-124b*, *miR-144*, *miR-199-s*, and *miR-104* were excluded from analysis in this study because individual Taqman MicroRNA Assays for these miRNAs are not available. In addition, expression levels of *miR-154*, *miR-211*, *miR-220*, *miR-302c*, and *miR-323* in OSCC cells were unevaluated because their expression in RT7 for normalization was undetermined by real-time RT-PCR analysis. Compared with expression levels in RT7, frequent up-regulation (>1.5-fold expression,  $\geq 66.7\%$  of OSCC lines) was found only in 11 of 148 (7.4%) miRNAs, whereas frequent down-regulation (<0.5-fold expression,  $\geq 66.7\%$  of OSCC lines) was observed in 54 of 148 (36.5%) miRNAs (Table 1), suggesting that some subsets of miRNAs are generally down-regulated in OSCC lines compared with normal oral keratinocytes.

**Methylation analysis of candidate miRNAs in OSCC cell lines.** We next searched the human genome database (University of California Santa Cruz Genome Bioinformatics)<sup>10</sup> for the existence

<sup>10</sup> <http://genome.ucsc.edu/>

of CpG islands around these 157 miRNA genes and confirmed that 21 miRNAs were located on/around (within 1,000 bp) CpG islands (Supplementary Table S4). Among those 21 miRNAs, we focused on *miR-34b*, *miR-132*, *miR-137*, *miR-193a*, and *miR-203* due to their frequent down-regulation in a panel of 18 OSCC cell lines: the percentage of OSCC lines with a remarkable down-regulation in these five miRNA genes compared with RT7 (<0.5-fold expression) were 100% (18 of 18), 72.2% (13 of 18), 72.2% (13 of 18), 72.2% (13 of 18), and 100% (18 of 18), respectively (Fig. 1C). The expression of the five miRNAs was restored by demethylation with 5-aza-dCyd at a high frequency in OSCC cells lacking their expressions (Supplementary Table S5), suggesting that aberrant DNA methylation suppressed expression of these five miRNAs.

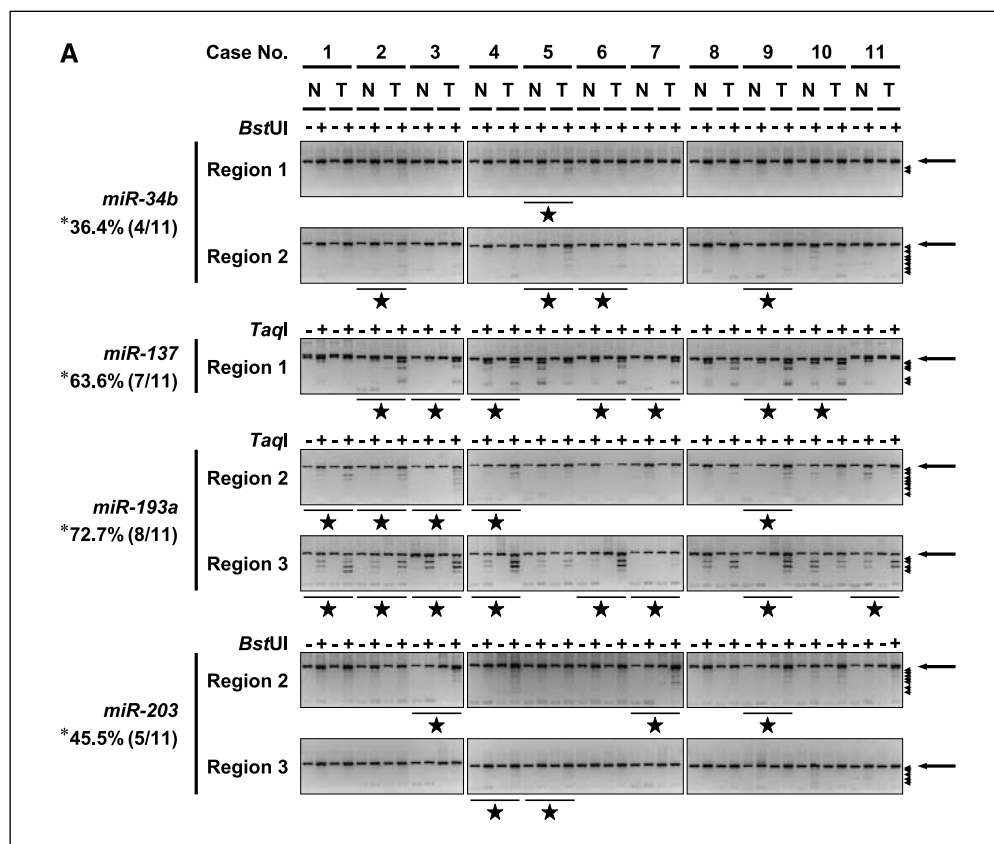
To determine the correlation between the DNA methylation status of these five miRNAs and their expression patterns in the 18 OSCC cell lines and RT7, we performed COBRA. The physical relationships between these miRNA genes, CpG islands, and the primers for COBRA are shown in Fig. 2A. Aberrant DNA methylation within CpG islands around *miR-34b*, *miR-137*, *miR-193a*, and *miR-203*, except *miR-132*, was detected in all of the OSCC lines having down-regulation of their expression (Fig. 2B). Consistent with the results of COBRA, aberrant DNA methylation was also shown by bisulfite sequencing in the OSCC lines lacking the expression of four candidate miRNAs but not in RT7 and the cell lines expressing these miRNAs (Fig. 2C). Therefore, we further analyzed *miR-34b*, *miR-137*, *miR-193a*, and *miR-203* as possible candidates.

**Methylation and expression analysis of selected miRNAs in primary OSCC cases.** To determine whether the methylation of the four miRNAs also occurs in primary OSCC tumors in a tumor-

specific manner, the correlation between DNA methylation status and expression patterns of the four genes in primary OSCCs with a corresponding noncancerous oral mucosa was examined using COBRA and Taqman real-time RT-PCR analysis, respectively. In COBRA, tumor-specific DNA methylation of *miR-34b*, *miR-137*, *miR-193a*, and *miR-203* was detected in 36.4% (4 of 11), 63.6% (7 of 11), 72.7% (8 of 11), and 45.5% (5 of 11) of primary OSCC cases, respectively (Fig. 3A). Positive cases of *miR-137* and *miR-193a* showed conspicuous fragments from methylated alleles in a tumor-specific manner. On the other hand, most of the positive cases of *miR-34b* and *miR-203* showed a trace of fragments from methylated alleles in tumor specimens, indicating that frequencies of aberrant methylation around *miR-34b* and *miR-203* in tumor cells were very low. Although there were a few cases in which restricted fragments from methylated alleles were observed in normal tissues, we considered tumor specimens, in which large amounts of restricted fragments from methylated alleles were more clearly detected compared with paired normal tissues, to be positive cases having tumor-specific hypermethylation.

In the Taqman real-time RT-PCR analysis, expression levels of *miR-34b*, *miR-137*, *miR-193a*, and *miR-203* in tumors compared with paired normal oral mucosa were reduced in 27.2% (3 of 11), 54.5% (6 of 11), 45.5% (5 of 11), and 63.6% (7 of 11) of primary OSCC cases, respectively (Fig. 3B). Consequently, both tumor-specific DNA methylation and down-regulated expression of *miR-34b*, *miR-137*, *miR-193a*, and *miR-203* were observed in 25% (1 of 4), 71.4% (5 of 7), 62.5% (5 of 8), and 40% (2 of 5) of primary OSCC cases, respectively; note that the denominator is the number of primary OSCC cases, in which restricted fragments from methylated alleles were detected by COBRA, and the numerator is the

**Figure 3.** Methylation and expression analyses in 11 primary OSCC cases. A, COBRA for candidate miRNA genes in surgically resected primary OSCC tumors (T) and corresponding noncancerous oral mucosa (N). Presence of restriction enzyme processing is indicated with plus or minus above the results of COBRA. Stars, cases in which tumor-specific methylation was detected. \*, frequencies of cases in which aberrant methylation of candidate miRNA was detected by COBRA.





number of primary OSCC cases, in which both DNA methylation around miRNA genes and down-regulation of their expressions were detected by COBRA and Taqman real-time RT-PCR analysis, respectively. Those results suggest that *miR-137* and *miR-193a* are most likely miRNAs frequently silenced through tumor-specific hypermethylation in OSCC. Bisulfite sequencing of those miRNAs in representative primary OSCC tumors clearly confirmed the results of COBRA (Fig. 3C). Therefore, it finally became our prime.

**Tumor-suppressive effects of *miR-137* and *miR-193a* on the growth of OSCC cell lines.** Because our expression and methylation analyses identified *miR-137* and *miR-193a* as candidate miRNAs silenced via tumor-specific hypermethylation in OSCC, we examined growth-inhibitory effects of *miR-137* or *miR-193a* through the transient transfection of double-strand RNA (dsRNA) mimicking either *miR-137* or *miR-193a* into OSCC cell lines lacking the expression of these two miRNAs. Restoration of *miR-137* or *miR-193a* expression significantly reduced cell growth in all of OSCC cell lines tested (Fig. 4A), suggesting that both *miR-137* and *miR-193a* have a tumor suppressor function in oral epithelia. In addition, we noticed that the apoptotic change was more serious in transfectants of *miR-193a* than those of *miR-137* under the phase-contrast microscope (Fig. 4A). At 72 h after transfection, a large number of transfectants of *miR-193a* were

rounded and floating compared with the control counterpart, whereas these morphologic changes were much weaker in transfectants of *miR-137*. In FACS analysis (Fig. 4B), 48 h after transfection of both *miR-137* or *miR-193a* resulted in a decrease in S and G<sub>2</sub>-M phase cells. Notably, *miR-137* mainly induced the accumulation of G<sub>0</sub>-G<sub>1</sub> phase cells, whereas *miR-193a* induced the accumulation of sub-G<sub>1</sub> phase cells, suggesting that *miR-137* and *miR-193a* might be predominantly associated with cell cycle arrest at the G<sub>1</sub>-S checkpoint and apoptotic change, respectively, in OSCC cells. Using the TUNEL assay, we tested whether these morphologic changes were caused by apoptosis. Twenty-four hours after the transfection of *miR-193a*, apoptotic cells were detected in both HSC-2 (Fig. 4C) and HO-1-N-1 (data not shown) cells but not clearly detected in transfectants of *miR-137* (data not shown). Moreover, we examined the effects of caspase inhibitors on *miR-193a*-induced reduction of cell growth in HSC-2 and HO-1-N-1 cells (Fig. 4D). Reduction of cell growth was partially but significantly inhibited by all three caspase inhibitors in both cells, suggesting that *miR-193a* may induce the reduction of cell growth at least in part through caspase-mediated apoptosis. In addition, effects of zDEVD-fmk or zVAD-fmk were more remarkable compared with zIETD-fmk in both cell lines, suggesting that activation of caspase-3, one of effector caspases, may be crucial in *miR-193a*-induced apoptosis in OSCC.

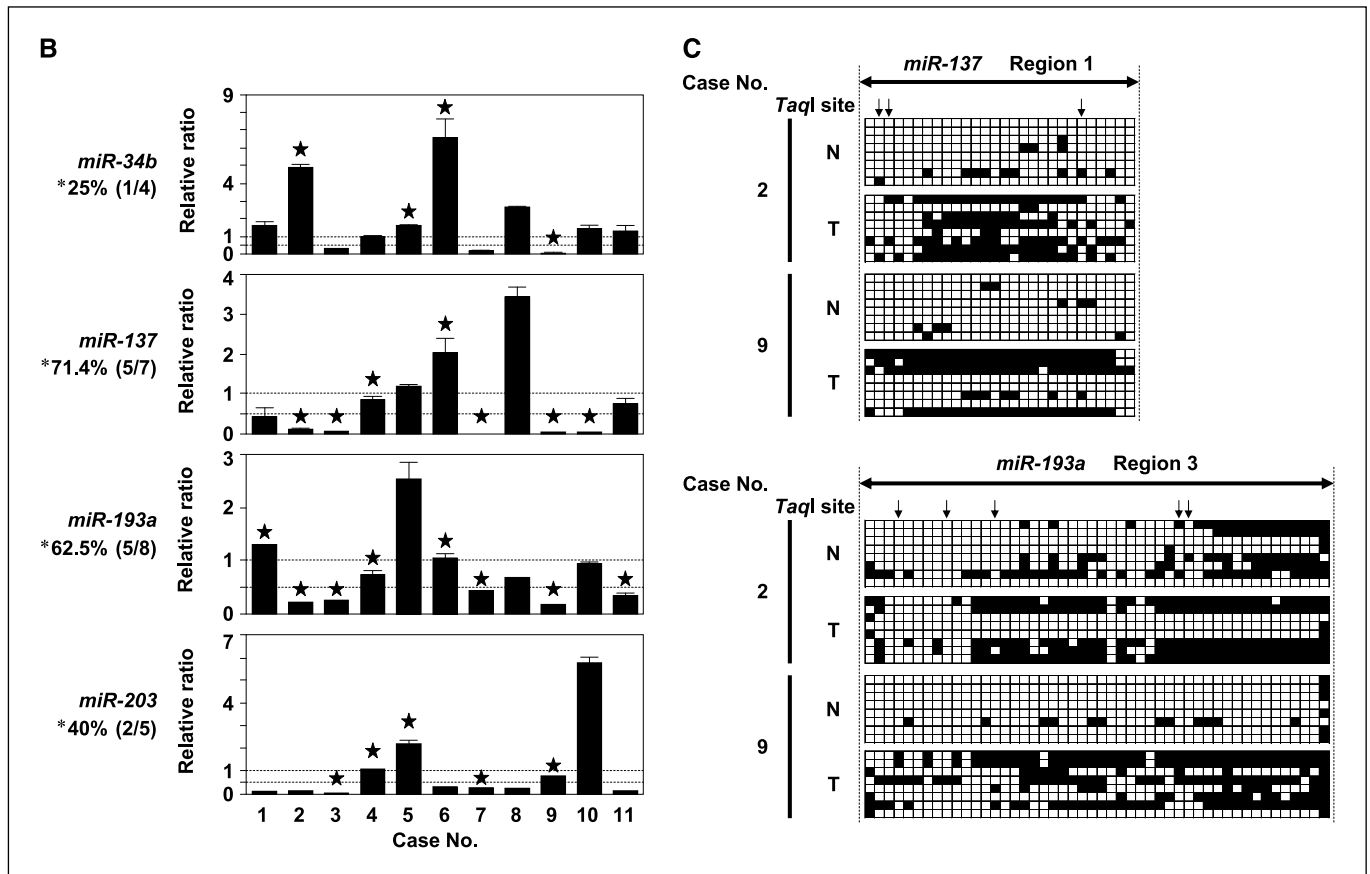


**Figure 3 Continued.** B, quantitative real-time RT-PCR analysis for expression levels of candidate miRNAs in primary OSCC tumors compared with paired normal oral mucosa. Stars, cases in which tumor-specific methylation was detected by COBRA. \*, frequencies of cases, in which a remarkable down-regulation of candidate miRNA expression (<0.5-fold expression) was observed compared with paired normal oral mucosa, among cases found to have the tumor-specific methylation by COBRA. C, results of bisulfite sequencing of representative cases. Horizontal bars with arrowheads, PCR product; vertical arrows, restriction enzyme sites. Open and filled squares represent unmethylated and methylated CpG sites, respectively, and each row represents a single clone.

### Screening of predicted targets of *miR-137* and *miR-193a*.

To explore oncogenic targets of *miR-137* or *miR-193a*, we focused on CDK6, E2F6, and NCOA2/TIF2 as *miR-137* targets, and E2F1, E2F6, KRAS, MCL1, MYCN, and PTK2/FAK as *miR-193a* targets according to computational prediction<sup>7-9</sup> and the reported function of predicted genes. We first performed Western blot analysis of these predicted targets 48 h after transfection of dsRNA

mimicking either *miR-137* or *miR-193a* into OSCC lines lacking the expression of these miRNAs (Fig. 5A). Protein expression levels of CDK6, E2F6, and NCOA2/TIF2 were clearly reduced in all *miR-137* transfectants compared with their control counterparts. In all *miR-193a* transfectants, protein levels of E2F6 and PTK2/FAK were remarkably decreased compared with their control counterparts. In addition, down-regulation of MCL1, an antiapoptotic

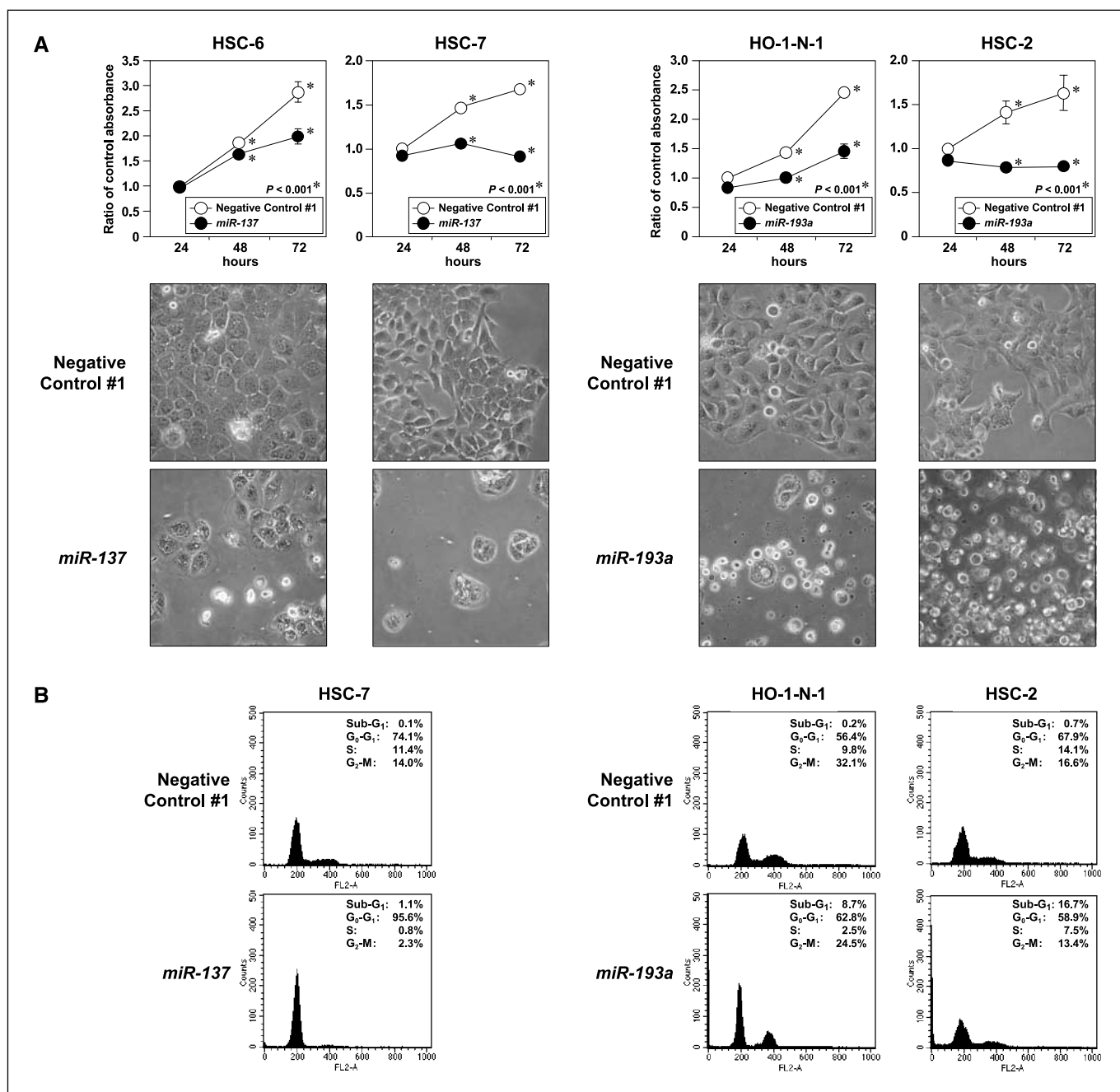


**Figure 4.** Tumor-suppressive effects of *miR-137* and *miR-193a* on OSCC cell lines lacking their expression. **A**, growth curves (top) and phase-contrast micrographs (bottom) of OSCC cell lines in which 10 nmol/L of Pre-miR miRNA Precursor Molecule mimicking *miR-137* or *miR-193a*, or control nonspecific dsRNA (Pre-miR Negative Control #1) was transfected using Lipofectamine RNAiMAX. The numbers of viable cells 24 to 72 h after transfection were assessed by WST assay. Points, mean of triplicate determinations in these experiments; bars, SE. Phase-contrast micrographs show the cells cultured for 72 h after transfection. \*,  $P < 0.05$ , statistical analysis used the Mann-Whitney  $U$  test. **B**, representative results of the population in each phase of cell cycle assessed by FACS using cell lines 48 h after transfection of Pre-miR miRNA Precursor Molecule mimicking *miR-137* or *miR-193a*, or Pre-miR Negative Control #1. Because HSC-6 cell line contains two different populations, diploid (2n) and tetraploid (4n) clones, which show complicated pattern in cell cycle analysis by FACS, we did not include this cell line for the analysis.



Bcl-2 family member, was also detected in all OSCC cell lines transfected with *miR-193a* compared with negative control dsRNA, although we found no noticeable differences in the protein levels of Bcl-2 and Bcl-X<sub>L</sub> between *miR-193a* and control transfectants. To further determine whether the predicted target sites against these two miRNAs in 3'-UTR of mRNAs of *CDK6*, *E2F6*, *MCL1*, *NCOA2/TIF2*, and *PTK2/FAK* (see Supplementary Table S3) were responsible for the translational regulation by dsRNA, we next performed luciferase assays with vectors containing these 3'-UTR target sites downstream of the *luciferase* reporter gene (Fig. 5B). The statistically significant reduction of luciferase activity was observed in NA cells cotransfected with *miR-137* and a reporter vector containing the *CDK6* 3'-UTR target site and those cotransfected with *miR-193a* and a vector containing the *E2F6* 3'-UTR target site compared with control transfectants. No notable alteration of luciferase activity was detected between *miR-137* or *miR-193a* transfectant and control counterpart in other genes. These data suggest that at least *CDK6* and *E2F6* are possible targets for *miR-137*-mediated and *miR-193a*-mediated translational

down-regulation in oral epithelia, respectively, and that activation of these molecules through methylation-mediated silencing of those two miRNAs may contribute to the pathogenesis of OSCC.

### Discussion

The present study clearly shows that an integrated and sequential approach using expression and methylation analyses makes it possible to efficiently identify tumor suppressor miRNAs silenced by tumor-specific DNA methylation in cancer cells. In our miRNA expression profiles of OSCC cell lines, 36.5% (54 of 148) of miRNAs were remarkably down-regulated, which is consistent with the previous reports that miRNA expression seemed globally lower in tumors than normal tissues (7, 23). These findings suggest that the global decrease in expression levels of miRNAs contributes to carcinogenesis through the activation of oncogenic pathways, which potential targets for these miRNAs might affect greatly. In addition, recent studies also showed that *miR-127* was decreased by aberrant alterations in

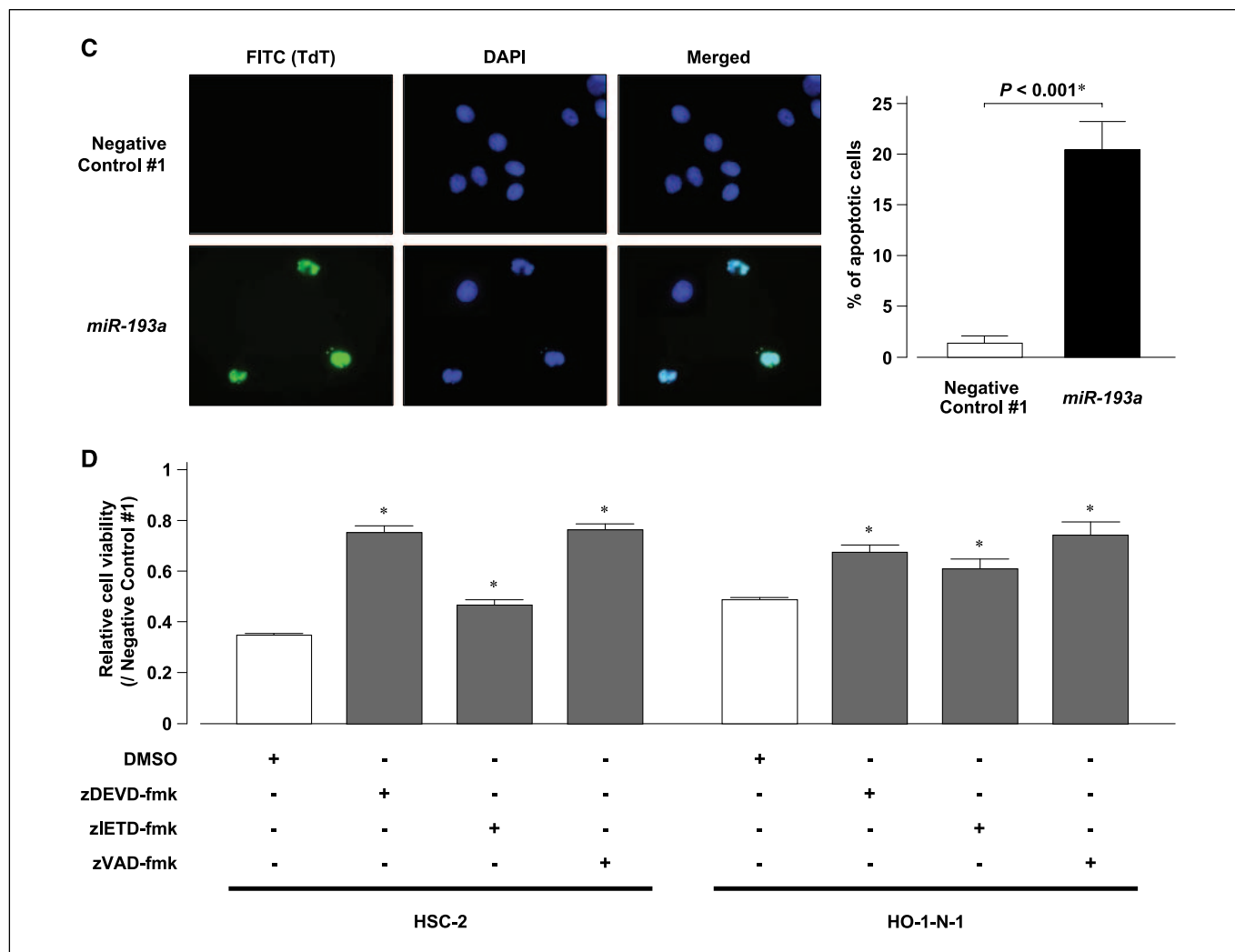


**Figure 4 Continued.** C, left, representative images of TUNEL staining in HSC-2 cells at 24 h after transfection of Pre-miR miRNA Precursor Molecule mimicking *miR-193a* or Pre-miR Negative Control #1 under the fluorescence microscope; right, quantitative analysis of apoptotic cells among HSC-2 cells 24 h after transfection of *miR-193a* or control nonspecific dsRNA under the fluorescence microscope. DAPI, 4',6-diamidino-2-phenylindole. D, effects of caspase inhibitors on cell growth in HSC-2 (left) and HO-1-N-1 (right) cell lines transfected with *miR-193a*. \*,  $P < 0.05$  versus vehicle-treated cells, statistical analysis used the Mann-Whitney  $U$  test.

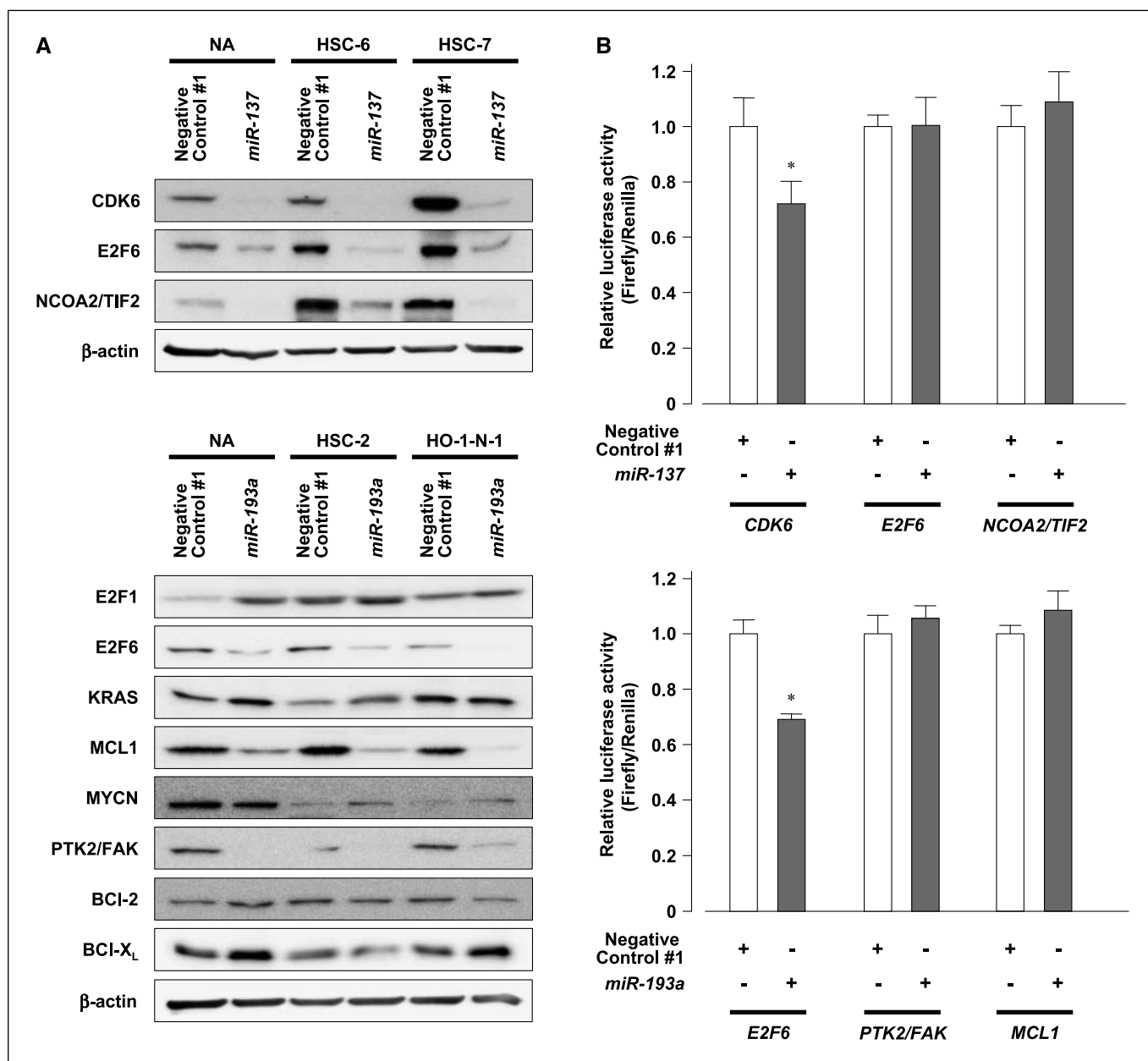


**Figure 5.** Screening of predicted targets of *miR-137* and *miR-193a*. **A**, representative results of Western blotting of predicted targets for *miR-137* or *miR-193a* in OSCC cell lines lacking expression of *miR-137* (NA, HSC-6, and HSC-7; top) or *miR-193a* (NA, HSC-2, and HO-1-N-1; bottom) 48 h after transfection of Pre-miR miRNA Precursor Molecule mimicking these two miRNAs, or control nonspecific dsRNA (Pre-miR Negative Control #1) using Lipofectamine RNAiMAX. **B**, luciferase assays of *miR-137*-nonexpressing and *miR-193a*-nonexpressing NA cells 48 h after cotransfection of pMIR-REPORT luciferase vectors containing 3'-UTR target sites of *CDK6*, *E2F6*, and *NCOA2/TIF2* for *miR-137* or those of *E2F6*, *PTK2/FAK*, and *MCL1* for *miR-193a* (see Supplementary Table S3), Pre-miR miRNA Precursor Molecule mimicking *miR-137* or *miR-193a*, respectively, or Pre-miR Negative Control #1, and pRL-hTK internal control vector using Lipofectamine 2000 (Invitrogen). \*,  $P < 0.05$  versus vehicle-treated cells, statistical analysis used the Mann-Whitney  $U$  test.

DNA methylation and histone modification in bladder cancer cells (12) and that *miR-124a* was inactivated by CpG island hypermethylation in several types of human cancers (11), suggesting tumor-specific DNA methylation to be an important molecular mechanism for the down-regulation of miRNA expression, similar to classic TSGs, in human cancers. Therefore, we were particular about a screening based on methylation analyses, and advanced the present study.

In the course of a program to screen a panel of 18 OSCC cell lines for tumor suppressor miRNAs silenced by aberrant DNA

methylation, we selected *miR-34b*, *miR-137*, *miR-193a*, and *miR-203* as possible candidate genes. Our data showed that these miRNA expressions were frequently decreased in OSCC cell lines and that treatment with 5-aza-dCyd restored their expression levels in cells lacking their expressions. Moreover, complete consistency in the correlation between DNA methylation status around these four genes and their expression patterns was confirmed in a panel of 18 OSCC cell lines, strongly suggesting that DNA methylation around CpG islands seemed to deregulate the expression of these genes in OSCC cell lines. Recently, *miR-34* family genes, including

*miR-34b*, were shown to be direct transcriptional targets of p53 (24), indicating that *miR-34b* may play a pivotal role in the p53 tumor suppressor network, although marked deregulation of the expression of *miR-34b* in human cancers has not been reported. The precise functions of *miR-137*, *miR-193a*, and *miR-203* have not been characterized, but a few studies indicated their abnormal expressions in human cancers. Decreases in *miR-137* expression were described in colorectal cancer (25), central nervous system tumor cell lines (26), and neuroblastoma (27), suggesting that *miR-137* may be a TSG. Although an increase in expression levels of *miR-193a* was found in a microarray analysis for human B-cell chronic lymphocytic leukemia (28), there has been no detailed report about the aberrant expression of *miR-193a* in human cancers thus far. Down-regulation of *miR-203* expression was described in central nervous system tumor cell lines (26) and thyroid anaplastic carcinoma (29), whereas its up-regulation was also shown in breast cancer (30), lung cancer (31), and colorectal cancer (25).

In analyses using primary OSCC cases with both tumors and paired normal tissues, *miR-34b* and *miR-203* were excluded from our list of possible candidate genes for two reasons: (a) frequencies of aberrant methylation around *miR-34b* and *miR-203* in tumor cells were very low and (b) frequencies of primary cases, in which down-regulation of these genes was consistent with tumor-specific hypermethylation around these genes, were very low. Although it was unknown why these frequencies were even lower in OSCC cases than in OSCC cell lines, hypermethylation around *miR-34b* and *miR-203* might be one of the aberrant epigenetic events in a process of establishment of cell lines *in vitro*. On the other hand, frequencies of primary OSCC cases, in which down-regulation of *miR-137* and *miR-193a* expression was consistent with tumor-specific hypermethylation around these genes, were relatively high, similar to results in OSCC cell lines. *miR-137* is located in chromosomal region 1p21.3, and loss of heterozygosity (LOH) in this region has been reported in meningioma (32), pheochromocytomas (33), and paraganglioma (34). LOH at 17q11.2, where *miR-193a* is located, has also been described in Barrett's esophageal tumors (35), neurofibromatosis 1 (36), ovarian adenocarcinoma (37), cervical carcinoma (38), and breast cancer (39). These previous studies indicated that TSGs mapped to these loci and that *miR-137* and *miR-193a* might be the targets of these losses. Moreover, we found that *miR-137* and *miR-193a* might be predominantly associated with cell cycle arrest at the G<sub>1</sub>-S checkpoint and apoptotic change, respectively, indicating that *miR-137* and *miR-193a* seem to have a tumor suppressor function in oral epithelia.

Here, we also showed that *miR-137* and *miR-193a* target *CDK6* and *E2F6*, respectively, in OSCC cell lines. *CDK6* regulates major cell cycle transitions as an oncogene and has been reported the potential target of *miR-124a*, which is epigenetically silenced in human cancers (11). *E2F6* is a transcriptional repressor in the E2F family (40), and its potential oncogenic capacity was also shown recently (41). Our Western blotting also showed that the protein levels of *E2F6* and *NCOA2/TIF2* were remarkably down-regulated in *miR-137* transfectants, and those of *MCL1* and *PTK2/FAK* were in *miR-193a* transfectants, although the inhibition of luciferase activity through a possible 3'-UTR target sequence of each gene inserted into downstream of the *luciferase* gene within reporter vectors was not observed in those target genes, suggesting a possible indirect target effect. *NCOA2/TIF2*, a member of the p160 family of coactivators, and *PTK2/FAK*, a member of cytoplasmic nonreceptor protein tyrosine kinases, have been described to be associated with human cancer development (42, 43). *MCL1* is an antiapoptotic Bcl-2 family protein, which contributes to cancer progression, resistance to chemotherapy, and poor clinical outcome (44). These results suggest that *miR-137* and *miR-193a* may induce the down-regulation of these proteins by either direct binding to their target mRNAs or their unknown indirect effects other than direct binding, resulting in cell cycle arrest at the G<sub>1</sub>-S checkpoint and apoptosis, respectively, in oral squamous cells.

In conclusion, our study showed for the first time that (a) tumor-specific hypermethylation in OSCC was an important molecular mechanism causing the global down-regulation of miRNAs, in a similar manner to that shown for classic TSGs; (b) *miR-137* and *miR-193a* were tumor suppressor miRNAs silenced by tumor-specific hypermethylation in OSCC, suggesting that the epigenetic silencing of these miRNAs plays a pivotal role during oral carcinogenesis; and (c) *CDK6* and *E2F6* were potential targets for *miR-137* and *miR-193a*, respectively.

## Acknowledgments

Received 9/6/2007; revised 1/23/2008; accepted 1/24/2008.

**Grant support:** Scientific Research and Scientific Research on Priority Areas, and a 21st Century Center of Excellence Program for Molecular Destruction and Reconstitution of Tooth and Bone from the Ministry of Education, Culture, Sports, Science, and Technology, Japan; Core Research for Evolutional Science and Technology of Japan Science and Technology Corp.; and New Energy and Industrial Technology Development Organization.

The costs of publication of this article were defrayed in part by the payment of page charges. This article must therefore be hereby marked *advertisement* in accordance with 18 U.S.C. Section 1734 solely to indicate this fact.

We thank Professor Masaki Noda (Hard Tissue Genome Research Center, Tokyo Medical and Dental University) for continuous encouragement throughout this work and Ayako Takahashi and Rumi Mori for technical assistance.

## References

- Bartel DP. MicroRNAs: genomics, biogenesis, mechanism, and function. *Cell* 2004;116:281-97.
- He L, Hannon G J. MicroRNAs: small RNAs with a big role in gene regulation. *Nat Rev Genet* 2004;5:522-31.
- Miska EA. How microRNAs control cell division, differentiation and death. *Curr Opin Genet Dev* 2005; 15:563-8.
- Harfe BD. MicroRNAs in vertebrate development. *Curr Opin Genet Dev* 2005;15:410-5.
- Esquela-Kerscher A, Slack FJ. Oncomirs—microRNAs with a role in cancer. *Nat Rev Cancer* 2006;6:259-69.
- Osada H, Takahashi T. MicroRNAs in biological processes and carcinogenesis. *Carcinogenesis* 2007;28: 2-12.
- Lu J, Getz G, Miska EA, Alvarez-Saavedra E, et al. MicroRNA expression profiles classify human cancers. *Nature* 2005;435:834-8.
- Calin GA, Dumitru CD, Shimizu M, et al. Frequent deletions and down-regulation of micro-RNA genes miR15 and miR16 at 13q14 in chronic lymphocytic leukemia. *Proc Natl Acad Sci U S A* 2002;99:15524-9.
- Calin G A, Croce CM. MicroRNAs and chromosomal abnormalities in cancer cells. *Oncogene* 2006;25:6202-10.
- Garzon R, Fabbri M, Cimmino A, Calin GA, Croce CM. MicroRNA expression and function in cancer. *Trends Mol Med* 2006;12:580-7.
- Lujambio A, Ropero S, Ballester E, et al. Genetic unmasking of an epigenetically silenced microRNA in human cancer cells. *Cancer Res* 2007;67:1424-9.
- Saito Y, Liang G, Egger G, et al. Specific activation of microRNA-127 with down-regulation of the proto-oncogene BCL6 by chromatin-modifying drugs in human cancer cells. *Cancer Cell* 2006;9:435-43.
- Parkin DM, Bray F, Ferlay J, Pisani P. Global cancer statistics, 2002. *CA Cancer J Clin* 2005;55:74-108.
- Nomura K, Sobue T, Nakatani H, et al. Number of deaths and proportional mortality rates from malignant neoplasms by site in Japan (2003). In: The Editorial Board of the Cancer Statistics in Japan. *Cancer statistics in Japan 2005*. Tokyo: National Cancer Center; 2005. p. 36-9.
- Scully C, Field JK, Tanzawa H. Genetic aberrations in oral or head and neck squamous cell carcinoma (SCCHN). 1. Carcinogen metabolism, DNA repair and cell cycle control. *Oral Oncol* 2000;36:256-63.
- Ha PK, Califano JA. Promoter methylation and

- inactivation of tumour-suppressor genes in oral squamous-cell carcinoma. *Lancet Oncol* 2006;7:77–82.
17. Snijders AM, Schmidt BL, Fridlyand J, et al. Rare amplicons implicate frequent deregulation of cell fate specification pathways in oral squamous cell carcinoma. *Oncogene* 2005;24:4232–42.
  18. Baldwin C, Garnis C, Zhang L, Rosin MP, Lam WL. Multiple microalterations detected at high frequency in oral cancer. *Cancer Res* 2005;65:7561–7.
  19. Liu CJ, Lin SC, Chen YJ, Chang KM, Chang KW. Array-comparative genomic hybridization to detect genome-wide changes in microdissected primary and metastatic oral squamous cell carcinomas. *Mol Carcinog* 2006;45:721–31.
  20. Nakaya K, Yamagata HD, Arita N, et al. Identification of homozygous deletions of tumor suppressor gene FAT in oral cancer using CGH-array. *Oncogene* 2007;26:5300–8.
  21. Suzuki E, Imoto I, Pimkhaokham A, et al. PRTFDC1, a possible tumor-suppressor gene, is frequently silenced in oral squamous-cell carcinomas by aberrant promoter hypermethylation. *Oncogene* 2007;26:7921–32.
  22. Xiong Z, Laird PW. COBRA: a sensitive and quantitative DNA methylation assay. *Nucleic Acids Res* 1997;25:2532–4.
  23. Thomson JM, Newman M, Parker JS, Morin-Kensicki EM, Wright T, Hammond SM. Extensive post-transcriptional regulation of microRNAs and its implications for cancer. *Genes Dev* 2006;20:2202–7.
  24. He L, He X, Lim LP, et al. A microRNA component of the p53 tumour suppressor network. *Nature* 2007;447:1130–4.
  25. Bandres E, Cubedo E, Agirre X, et al. Identification by real-time PCR of 13 mature microRNAs differentially expressed in colorectal cancer and non-tumoral tissues. *Mol Cancer* 2006;5:29.
  26. Gaur A, Jewell DA, Liang Y, et al. Characterization of microRNA expression levels and their biological correlates in human cancer cell lines. *Cancer Res* 2007;67:2456–68.
  27. Chen Y, Stallings RL. Differential patterns of microRNA expression in neuroblastoma are correlated with prognosis, differentiation, and apoptosis. *Cancer Res* 2007;67:976–83.
  28. Calin GA, Liu CG, Sevignani C, et al. MicroRNA profiling reveals distinct signatures in B cell chronic lymphocytic leukemias. *Proc Natl Acad Sci U S A* 2004;101:11755–60.
  29. Visone R, Pallante P, Vecchione A, et al. Specific microRNAs are down-regulated in human thyroid anaplastic carcinomas. *Oncogene* 2007;26:7590–5.
  30. Iorio MV, Ferracin M, Liu CG, et al. MicroRNA gene expression deregulation in human breast cancer. *Cancer Res* 2005;65:7065–70.
  31. Yanaihara N, Caplen N, Bowman E, et al. Unique microRNA molecular profiles in lung cancer diagnosis and prognosis. *Cancer Cell* 2006;9:189–98.
  32. Bello MJ, de Campos JM, Vaquero J, et al. High-resolution analysis of chromosome arm 1p alterations in meningioma. *Cancer Genet Cytogenet* 2000;120:30–6.
  33. Aarts M, Dannenberg H, de Leeuw RJ, et al. Microarray-based CGH of sporadic and syndrome-related pheochromocytomas using a 0.1–0.2 Mb bacterial artificial chromosome array spanning chromosome arm 1p. *Genes Chromosomes Cancer* 2006;45:83–93.
  34. Edstrom E, Mahlamaki E, Nord B, et al. Comparative genomic hybridization reveals frequent losses of chromosomes 1p and 3q in pheochromocytomas and abdominal paragangliomas, suggesting a common genetic etiology. *Am J Pathol* 2000;156:651–9.
  35. Swift A, Risk JM, Kingsnorth AN, Wright TA, Myskow M, Field JK. Frequent loss of heterozygosity on chromosome 17 at 17q11.2–q12 in Barrett's adenocarcinoma. *Br J Cancer* 1995;71:995–8.
  36. Kluwe L, Friedrich RE, Mautner VF. Allelic loss of the NF1 gene in NF1-associated plexiform neurofibromas. *Cancer Genet Cytogenet* 1999;113:65–9.
  37. Arnold JM, Huggard PR, Cummings M, Ramm GA, Chenevix-Trench G. Reduced expression of chemokine (C-C motif) ligand-2 (CCL2) in ovarian adenocarcinoma. *Br J Cancer* 2005;92:2024–31.
  38. Zijlmans HJ, Fleuren GJ, Baelde HJ, Eilers PH, Kenter GG, Gorter A. The absence of CCL2 expression in cervical carcinoma is associated with increased survival and loss of heterozygosity at 17q11.2. *J Pathol* 2006;208:507–17.
  39. Pierga JY, Reis-Filho JS, Cleator SJ, et al. Microarray-based comparative genomic hybridisation of breast cancer patients receiving neoadjuvant chemotherapy. *Br J Cancer* 2007;96:341–51.
  40. Wong CF, Barnes LM, Smith L, Popa C, Serewko-Auret MM, Saunders NA. E2F6: a member of the E2F family that does not modulate squamous differentiation. *Biochem Biophys Res Commun* 2004;324:497–503.
  41. Chen C, Wells AD. Comparative analysis of E2F family member oncogenic activity. *PLoS ONE* 2007;2:e912.
  42. Agoulnik IU, Vaid A, Nakka M, et al. Androgens modulate expression of transcription intermediary factor 2, an androgen receptor coactivator whose expression level correlates with early biochemical recurrence in prostate cancer. *Cancer Res* 2006;66:10594–602.
  43. Mitra SK, Hanson DA, Schlaepfer DD. Focal adhesion kinase: in command and control of cell motility. *Nat Rev Mol Cell Biol* 2005;6:56–68.
  44. Youle RJ, Strasser A. The BCL-2 protein family: opposing activities that mediate cell death. *Nat Rev Mol Cell Biol* 2008;9:47–59.